ceramics

MDPI

Article

Calcium Phosphate Powder Synthesized from Calcium Acetate and Ammonium Hydrophosphate for Bioceramics Application

Tatiana Safronova [1,2,*], Valery Putlayev [1,2], Yaroslav Filippov [2,3], Tatiana Shatalova [1,2], Evgeny Karpushkin [1], Dmitrii Larionov [2], Gilyana Kazakova [2] and Yury Shakhtarin [1]

1 Department of Chemistry, Lomonosov Moscow State University, Leninskie Gory, 1, Moscow 119991, Russia; valery.putlayev@gmail.com (V.P.); shatalovatb@gmail.com (T.S.); eukarr@gmail.com (E.K.); sh14101998@yandex.ru (Y.S.)

2 Materials Science Department, Lomonosov Moscow State University, Leninskie Gory, 1, Moscow 119991, Russia; filippovya@gmail.com (Y.F.); dmiselar@gmail.com (D.L.); gilyanakk@gmail.com (G.K.)

3 Research Institute of Mechanics, Lomonosov Moscow State University, Michurinskii pr., 1, Moscow 119192, Russia

* Correspondence: t3470641@yandex.ru; Tel.: +7-916-3470641

Received: 25 October 2018; Accepted: 11 December 2018; Published: 15 December 2018

Abstract: Calcium phosphate powder was synthesized at room temperature from aqueous solutions of ammonium hydrophosphate and calcium acetate without pH adjusting at constant Ca/P molar ratio 1.5. Phase composition of the as-synthesized powder depended on the precursors concentration: At 2.0 M of calcium acetate in the starting solution, poorly crystallized hydroxyapatite was formed, 0.125 M solution of calcium acetate afforded brushite, and the powders synthesized from 0.25–1.0 M calcium acetate solutions were mixtures of the mentioned phases. Firing at 1100 °C led to complete elimination of the reaction by-products, yet the phase composition of the annealed compacted samples was the following: When 2.0 M solution of calcium acetate was used, the obtained ceramics consisted of β-$Ca_3(PO_4)_2$, whereas at 0.125 to 1.0 M of calcium acetate, the ceramics was a mixture of β-$Ca_3(PO_4)_2$ and β-$Ca_2P_2O_7$. Synthesized calcium phosphate powders can be used as the powdered precursors for biocompatible bioresorbable composite ceramics production.

Keywords: hydroxyapatite; brushite; precipitation; tricalcium phosphate; calcium pyrophosphate; ceramic composite

1. Introduction

Ceramic materials based on calcium phosphates are widely used for bone implant production [1,2], since their chemical composition is identical to the inorganic component of bone tissue, hydroxyapatite (HA, $Ca_{10}(PO_4)_6(OH)_2$). Synthetic powders with desired properties including phase composition and particle size distribution are demanded for the fabrication of high-quality ceramics [3]. Precipitation of calcium phosphates powder from aqueous solution is the most popular and convenient synthetic approach to the nanosized particles [4]. The phase composition, morphology, and particle size distribution of the so prepared synthetic calcium phosphates strongly depend on a set of interrelated parameters such as pH, temperature, Ca/P ratio, and the components concentration in the reaction zone [5–8]. The choice of the pair of precursors (water-soluble substances containing Ca^{2+} and HPO_4^{2-} ions, respectively) is an additional factor governing the phase composition and quality of calcium phosphates powders and the ceramics based on them [9]. The most popular pairs of precursors for the synthesis of calcium phosphates powders for ceramics production include $Ca(OH)_2/H_3PO_4$ [10,11] and $Ca(NO_3)_2/(NH_4)_2HPO_4$ [8,12,13]. Besides the target calcium phosphate

compounds (i.e., hydroxyapatite or brushite), the interaction of these precursors yields certain by-products (NH_4NO_3 or H_2O) which can be removed from the powder compact or semi-finished item via heat treatment at relatively low temperature and therefore do not affect the sintering process occurring at temperatures above 500 °C [7].

There are other pairs of precursors exhibiting the same feature, formation of the by-products that can be completely removed from the calcium phosphates powder via the heat treatment prior to sintering. Obviously, the HPO_4^{2-} ions can be provided by phosphoric acid or by ammonium hydrophosphates. A variety of calcium compounds, such as $CaCO_3$ [14], $Ca(OH)_2$ [10,11], $CaCl_2$ [15,16], $Ca(NO_3)_2$ [7,8,13,16,17], and the carboxylic acids salts (calcium formate [18], calcium acetate [16,19,20], calcium propionate [21–23], calcium lactate [24,25], or calcium saccharates [26,27]) can be used as the source of Ca^{2+} ions. Most of the listed carboxylic acids or their salts are used as pH regulators in the food industry [28]; furthermore, these carboxylates, ammonium, and (hydro)phosphate ions are known as components of aqueous buffer solutions [29]. This fact can be exploited in the development of novel convenient methods of obtaining the powders for calcium phosphate ceramics production. It should be noted that calcium acetate is the most used calcium carboxylate for calcium phosphate synthesis as the source of Ca^{2+} ions. According to Equations (1) and (2), the interaction of $Ca(CH_3COO)_2$ and $(NH_4)_2HPO_4$ during calcium phosphates synthesis affords acetic acid and/or ammonium acetate as the reaction by-products:

$$Ca(CH_3COO)_2 + (NH_4)_2HPO_4 \rightarrow CaHPO_4{\cdot}2H_2O + 2CH_3COONH_4, \quad (1)$$

$$3Ca(CH_3COO)_2 + 2(NH_4)_2HPO_4 + xH_2O \rightarrow Ca_9(HPO_4)(PO_4)_5(OH) + 4CH_3COONH_4 + CH_3COOH. \quad (2)$$

It is worth mentioning that the phase composition of the ceramics based on the calcium phosphate powders (prepared in turn via the interaction of calcium acetate and ammonium hydrophosphate in an aqueous solution without pH adjusting) is affected by the precursors concentrations and ratio used in the calcium phosphate synthesis [16,19]. In detail, calcium phosphates powders synthesized from 0.5 M $Ca(CH_3COO)_2$ and 0.5 M $(NH_4)_2HPO_4$ aqueous solutions (at Ca/P = 1) [16] and from 2.0 M $Ca(CH_3COO)_2$ and 1.33 M $(NH_4)_2HPO_4$ (at Ca/P = 1.5) [19] contained low-crystalline hydroxyapatite and amorphous phases. However, phase composition of the ceramic materials after firing at 1100 °C was different: $Ca_2P_2O_7 + Ca_3(PO_4)_2$ in the former case [16] and $Ca_3(PO_4)_2 + Ca_{10}(PO_4)_6(OH)_2$ in the latter case [19]. These examples show that phase composition of the as-synthesized and fired calcium phosphates depends on the precursors concentrations in the reaction mixture. However, to the best of our knowledge, this effect has not been systematically considered so far.

In order to fill in the gap, we investigated the interaction between calcium acetate and ammonium hydrophosphate (aqueous solution, Ca/P = 1.5, no pH adjusting), the calcium acetate concentration varying between 0.125 and 2.0 M, with the focus on the phase composition of the formed calcium phosphates powders and the derived sintered ceramic. The obtained knowledge is a strong basis for the development of a convenient yet versatile procedure to prepare a powdered precursor of calcium phosphate ceramics with desirable phase composition.

2. Materials and Methods

2.1. pH Measurement in the Reaction Zone

To experimentally monitor the conditions in the reaction zone, 40 mL of an aqueous solution of $(NH_4)_2HPO_4$ (see the concentrations in Table 1) was added in 1 mL portions to 40 mL of an aqueous solution of $Ca(CH_3COO)_2$, and the pH was measured at 25 °C using a T50 computer-controlled automated titration system (Mettler Toledo AG, Schwerzenbach, Switzerland).

2.2. Calculation of pH in the Reaction Zone

pH profiles and concentrations of the crystalline phases in the reaction zone at 25 °C during portionwise (1 mL) addition of 140 mL of an aqueous solution of $(NH_4)_2HPO_4$ to 100 mL of an aqueous solution of $Ca(CH_3COO)_2$ were calculated using Visual MINTEQ 3.1 software (KTH Royal Institute of Technology, Stockholm, Sweden) [30] based on the simulation of ionic equilibria. The solutions concentrations were set as follows: 0.083 M $(NH_4)_2HPO_4$/0.125 M $Ca(CH_3COO)_2$ (case 1) and 0.667 M $(NH_4)_2HPO_4$/1.0 M $Ca(CH_3COO)_2$ (case 2). The allowed crystalline phases were hydroxyapatite $Ca_{10}(PO_4)_6(OH)_2$ (H), amorphous calcium phosphates $Ca_3(PO_4)_2$ (A), octacalcium phosphate $Ca_8H_2(PO_4)_6{\cdot}5H_2O$ (O), and brushite $CaHPO_4{\cdot}2H_2O$ (B).

Table 1. Concentration of solutions [1] used for powders synthesis at Ca/P = 1.5 and room temperature.

# of Synthesis	Labelling	Concentration of $Ca(CH_3COO)_2$ Aqueous Solution, M	Concentration of $(NH_4)_2HPO_4$ Aqueous Solution, M
1	2 M	2.000	1.333
2	1 M	1.000	0.667
3	0.5 M	0.500	0.333
4	0.25 M	0.250	0.167
5	0.125 M	0.125	0.083

[1] Volumes of $Ca(CH_3COO)_2$ and $(NH_4)_2HPO_4$ solutions were equal in the every synthesis.

2.3. Powder Synthesis and Sample Preparation

Calcium phosphate powder was fabricated via the conventional wet-precipitation technique. In detail, an aqueous solution of ammonium hydrophosphate $(NH_4)_2HPO_4$ (CAS number 7783-28-0, Sigma-Aldrich, St. Louis, MO, USA, puriss. p.a. ≥99%) was gradually added to an aqueous solution of stoichiometric (Equation (2)) amount of calcium acetate hydrate (CAS number 114460-21-8, Sigma-Aldrich, puriss. p.a. ≥99%). The investigated samples are listed in Table 1.

The formed white precipitate was matured under the mother liquor for 15 min at room temperature, filtered off, and dried in air for about 1 week (no washing of the precipitate was performed). The dried powder was disaggregated in a ball mill for 15 min in acetone medium, the liquid (acetone):powder:grinding medium (ZrO_2) ratio of 2:1:5 (*w*/*w*/*w*).

The so processed powder was sieved (Saatilene HiTechTM polyester fabrics, 200 μm) and uniaxially compacted portionwise (0.3 g) in a stainless-steel disc-shaped mold (diameter 12 mm) at 100 MPa using Carver laboratory press model C (USA) without additional plasticizer. The compacted specimens were heated to 1100 °C at 5 °C/min rate and annealed at that temperature for 2 h in air.

Since the precursors concentration was the only synthetic variable altered in the preparation of the powders discussed in this paper, the concentration of calcium acetate will be used throughout the text to indicate the particulate sample, for the sake of brevity. For example, the "0.5 M" powder will be aliased to the calcium phosphates powder synthesized as described above using the 0.5 M aqueous solution of calcium acetate as the starting component, etc.

2.4. Characterization of Samples

Density of the green compacts and sintered samples was calculated from the measured mass and geometry dimensions of the specimens. Particle size distribution was determined using a Laser Analyzer of Particles: Analizette 22 MicroTech Plus (Fritsch GmbH, Idar-Oberstein, Germany). Phase composition of the prepared powders and heat-treated compacted samples was examined by means of X-ray diffraction (XRD) (2θ 5–70°, Cu K_a radiation, Rigaku D/MAX 2500 (Rigaku Corporation, Tokyo, Japan) with rotating anode, Japan). The phases were identified using the ICDD PDF2 database [31]. The content of phases in the samples of ceramic material after calcination at 1100 °C for 2 h was determined from quantitative X-ray diffraction analysis according to a procedure

based on a standard method. According to this method the proportions of tricalciumphosphate and pyrophosphate can be quantified using XRD from integrated intensities of characteristic diffraction peaks. Thermal analysis (TA) was performed using an STA 409 PC Luxx thermal analyzer (NETZSCH, Selb, Germany) during heating in air (10 °C/min, 40–1000 °C), the specimen mass being at least 10 mg. The evolved gases composition was simultaneously monitored during the TA experiment using a coupled QMS 403C Aeolos quadrupole mass spectrometer (NETZSCH, Germany). The mass spectra were registered for the species with the following m/z values: 18 (corresponding to H_2O), 44 (corresponding to CO_2) and 30 (corresponding to NO). The specimens' microstructure was studied using a SUPRA 50 VP scanning electron microscope (Carl Zeiss, Oberkochen, Germany); the imaging was performed in a low vacuum mode at an accelerating voltage of 21 kV (VPSE secondary electron detector) or of 3–21 kV (SE2 detector).

3. Results and Discussion

Experimental and calculated curves showing the change in the reaction zone pH during portionwise addition of a solution of $(NH_4)_2HPO_4$ to that of $Ca(CH_3COO)_2$ are presented in Figures 1 and 2, respectively.

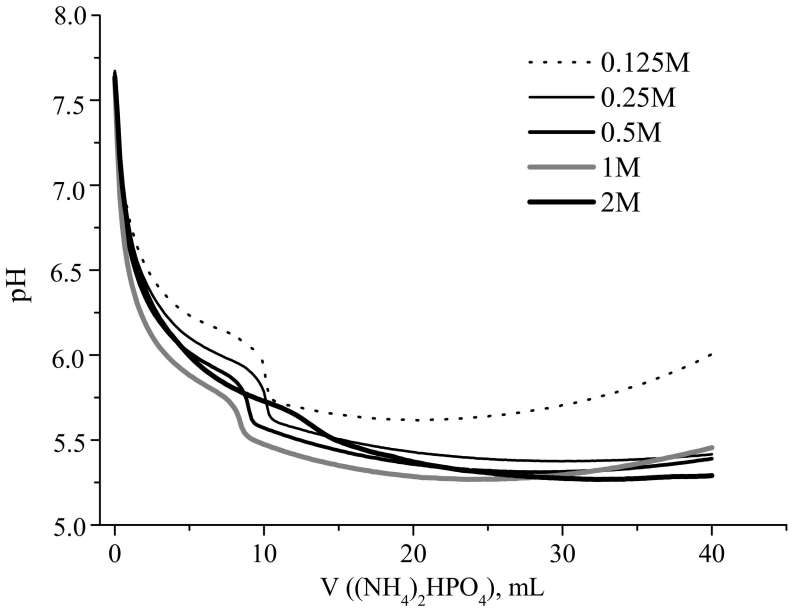

Figure 1. Change in the reaction zone pH during addition of aqueous solution of $(NH_4)_2HPO_4$ to that of $Ca(CH_3COO)_2$ to the final Ca/P ratio of 1.5. Concentrations of the $Ca(CH_3COO)_2$ solutions are shown in the legend.

Both dependences were strongly nonlinear, revealing a sharp decrease in the pH after the addition of the first portions of the ammonium hydrophosphate solution. For example, the addition of 2 mL of ammonium hydrophosphate solution resulted in the decrease in pH from 7.6 to about 6.15, and 6.5 for starting calcium acetate concentrations of 1 and 0.125 mol/L, respectively (Figure 1). The obtained calculated curves showed the pH drop from 9.1 to 6.8 at the corresponding point (Figure 2). The sharp decrease in the pH level in the beginning of the synthesis can be explained by the formation of amorphous calcium phosphate $Ca_3(PO_4)_2$ (type I, ACP1 [32,33]) or hydroxyapatite $Ca_{10}(PO_4)_6(OH)_2$ which have a positive or zero saturation index according to the calculation.

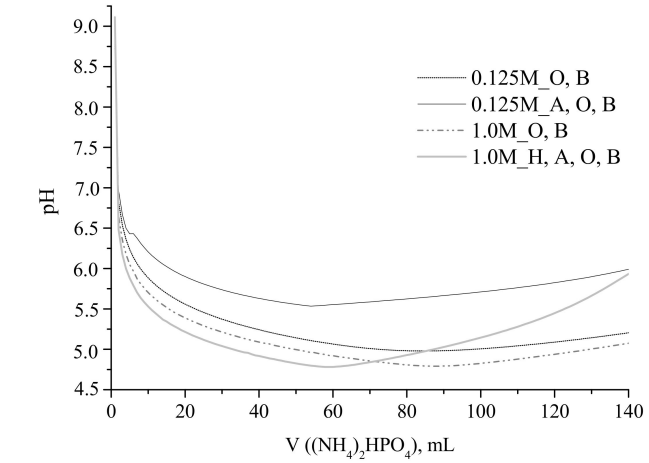

(**a**)

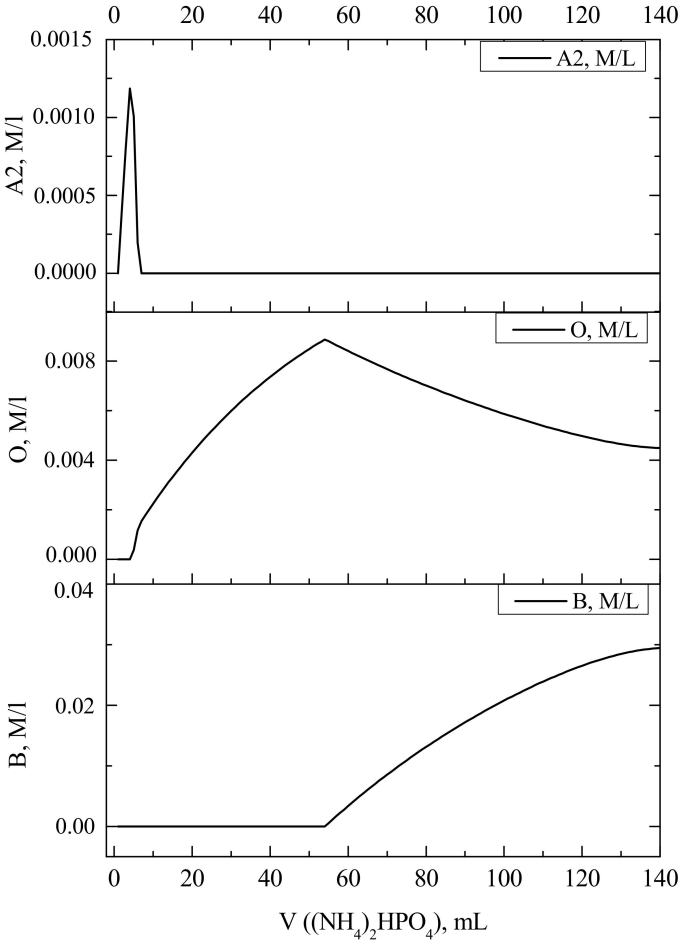

(**b**)

Figure 2. Calculated pH curves during addition of 0.083 and 0.667 M $(NH_4)_2HPO_4$ solutions to 100 mL of 0.125 and 1.0 M $Ca(CH_3COO)_2$ solutions respectively (**a**) and concentrations of the crystalline phases corresponding to the "0.125 M_A,O,B" line (**b**). The allowed crystalline phases were hydroxyapatite $Ca_{10}(PO_4)_6(OH)_2$ (H), amorphous calcium phosphates $Ca_3(PO_4)_2$ (A), octacalcium phosphate $Ca_8H_2(PO_4)_6{\cdot}5H_2O$ (O), and brushite $CaHPO_4{\cdot}2H_2O$ (B).

It should be noted that the experimental pH curves obtained for the solutions with $Ca(CH_3COO)_2$ concentration of 0.125 to 1.0 M were similar in the presence of the sharp second pH drop. In particular, the addition of 6–11 mL of $(NH_4)_2HPO_4$ solution resulted in the pH decrease from 5.79 to 5.44 (1 M calcium acetate), from 5.92 to 5.56 (0.5 M), from 5.98 to 5.6 (0.25 M), and from 6.14 to 5.69 (0.125 M). The pH curve for 2 M $Ca(CH_3COO)_2$ solution was much smoother, exhibiting gradual decrease in the pH between the starting and the final (40 mL) points, with an inflection around 12.5 mL of the added $(NH_4)_2HPO_4$ solution. After addition of half of the stoichiometric (according to Equation (2)) amount of the $(NH_4)_2HPO_4$ solution (20 mL), the experimental curves (except for that for 2 M calcium acetate solution) showed a slight increase in the pH (Figure 1). The calculated saturation index for brushite $CaHPO_4{\cdot}2H_2O$ (B) became positive after the addition of about half of the stoichiometric amount of $(NH_4)_2HPO_4$ solution (50 mL, Figure 2). The measured pH in the reaction zone ranged between 6.4 and 5.3 for the studies experimental cases.

From the set of the calculated pH profiles, only that for 0.125 M $Ca(CH_3COO)_2$ solution with amorphous calcium phosphates $Ca_3(PO_4)_2$ (A), octacalcium phosphate $Ca_8H_2(PO_4)_6{\cdot}5H_2O$ (O), and brushite $CaHPO_4{\cdot}2H_2O$ (B) as the allowed crystal phases showed the second pH drop similar to those for the experimental curves recorded at calcium acetate concentrations of 0.125 to 1.0 M. That drop could be assigned to the change in the saturation index for octacalcium phosphate $Ca_8H_2(PO_4)_6{\cdot}5H_2O$ (O) from negative to positive, corresponding to the maximum in the curve of the ACP2 content. A similar drop in the experimental pH curve has been earlier observed during the interaction between 7.5 mM K_2HPO_4 and 10 mM $CaCl_2$ aqueous solutions [32]. The obtained data have been ascribed to the competition of two reactions: The formation of ACP2 causing the release of H^+ into the solution and dissolution of ACPI accompanied by the consumption of H^+ ions. A similar experimental pH curve has been earlier observed during the interaction between of solutions of sodium phosphate ([NaOH]/[H_3P0_4] molar ratio approx. 1.75, pH 7.4) and calcium chloride $CaCl_2$ aqueous solutions [34].

As mentioned above, the experimental pH curves obtained at calcium acetate starting concentrations of 0.125–1 M demonstrated the increase in the pH value after addition of about half of stoichiometric amount of $(NH_4)_2HPO_4$ (Figure 1). That fact was attributed to the increase in the concentration of brushite crystalline phase, as confirmed by the calculated profiles of pH and concentration of crystalline phases (Figure 2). In contrast, the experimental pH curve obtained for 2 M aqueous solution of $Ca(CH_3COO)_2$ did not exhibit any pH increase. Hence, we concluded that the formation of brushite was suppressed in the latter case, obviously due to the buffering action of CH_3COONH_4 formed in fairly high concentration.

According to XRD data (Figure 3), the powder synthesized from most concentrated (2 M) aqueous solution of $Ca(CH_3COO)_2$ consisted of low-crystalline calcium phosphate with XRD reflexes which could be attributed to hydroxyapatite $Ca_{10}(PO_4)_6(OH)_2$ (PDF card # 9-432). The powder synthesized from the most dilute (0.125 M) aqueous solution of $Ca(CH_3COO)_2$ consisted majorly of brushite $CaHPO_4{\cdot}2H_2O$ (PDF card # 9-77). The "0.25 M", "0.5 M", and "1.0 M" powders contained both brushite $CaHPO_4{\cdot}2H_2O$ (PDF card # 9-77) and hydroxyapatite $Ca_{10}(PO_4)_6(OH)_2$, (PDF card # 9-432). It should be noted that the lower concentration of calcium acetate in the aqueous solution (and, hence, that of ammonium hydrophosphate) used for the synthesis resulted in less apparent signals of hydroxyapatite in the XRD patterns. Overall, the XRD data coincided with the data of pH measurements.

SEM images of the synthesized powders are collected in Figure 4. It can be seen that the observed particles morphology was in agreement with the XRD data. In detail, when more dilute solutions were used for the synthesis, the brushite signals in the XRD pattern were more apparent (Figure 3) and more plate-shaped particles were observed in the microscopy images (Figure 4). Particle size distributions for synthesized powders after disaggregation are presented in Figure 5. The integral carvers (Figure 5a) form two groups of lines: One group for more concentrated starting solutions of $Ca(CH_3COO)_2$ with concentrations of 1 and 2 M, and another for more dilute starting solutions of $Ca(CH_3COO)_2$ with concentrations of 0.5, 0.25 and 0.125 M. Particle size distributions obviously connected with the difference in morphology of particles with different phase composition of synthesized powders

(Figure 3) and with the quantity of synthesis by-product, which can be estimated from thermal analysis data (Figure 6). Sizes of particle aggregates (Figure 5b), as one can see at differential carvers, are in the interval of 0.5–175 μm for powder synthesized from 2.0 M solution of $Ca(CH_3COO)_2$, 0.4–100 μm for powder synthesized from 0.5 M solution of $Ca(CH_3COO)_2$, 0.5–70 μm for powder synthesized from 0.125 M solution of $Ca(CH_3COO)_2$. Larger aggregates are in powders synthesized from more concentrated starting solutions with higher content of calcium deficient hydroxyapatite and with higher content of reaction by-products including ammonium acetate CH_3COONH_4 and acetic acid CH_3COOH. The opportunity to form slight amounts of imine resin exists during disaggregation of synthesized powders in acetone in presence of NH_4^+ [35]. In addition, we guess that imine resin can bind the individual particles of calcium phosphates together to form bigger aggregates. The bonding effect of imine resin is more apparent for powders synthesized from more concentrated solutions. In spite of the smaller dimensions of individual particles of calcium deficient hydroxyapatite $Ca_9(HPO_4)(PO_4)_5(OH)$ than dimensions of individual particles of $CaHPO_4 \cdot 2H_2O$ (Figure 4), the most probable size of the aggregates for powder synthesized from 2.0 M (21 μm) solution of $Ca(CH_3COO)_2$ is higher than for powder synthesized from 0.125 M (10 μm) solution of $Ca(CH_3COO)_2$.

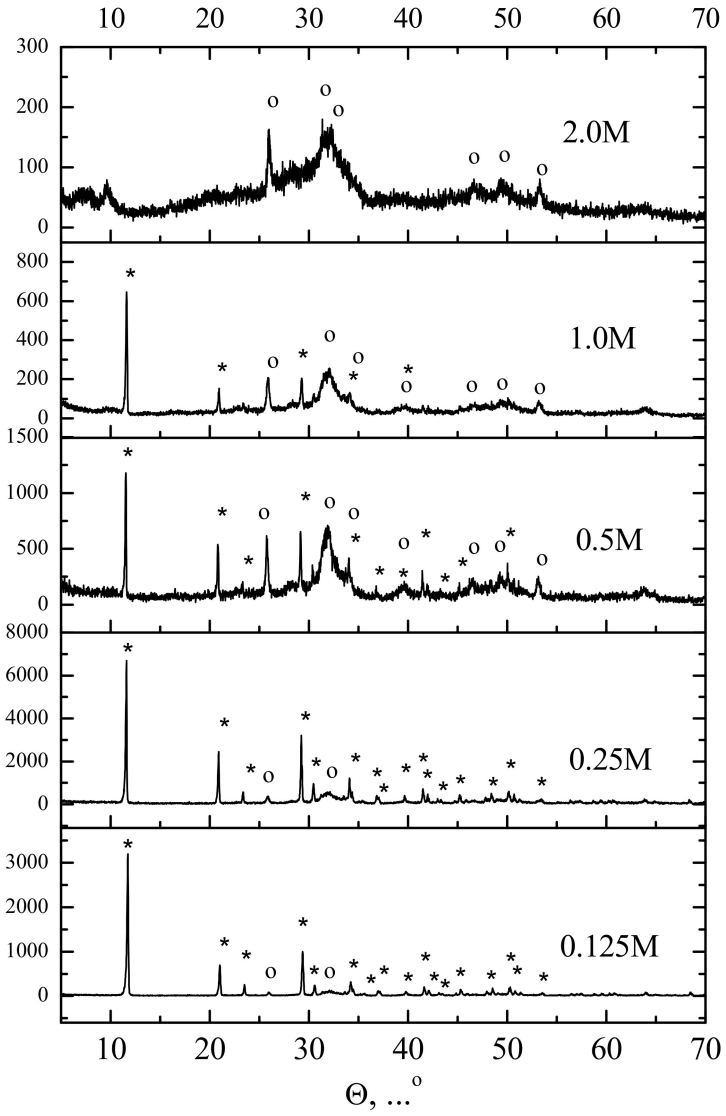

Figure 3. XRD patterns of the powders synthesized from aqueous solutions of $Ca(CH_3COO)_2$ of different concentrations (shown near the curves) and $(NH_4)_2HPO_4$ at Ca/P = 1.5. o—$Ca_{10}(PO_4)_6(OH)_2$, PDF card # 9-432; *—brushite $CaHPO_4 \cdot 2H_2O$, PDF card # 9-77.

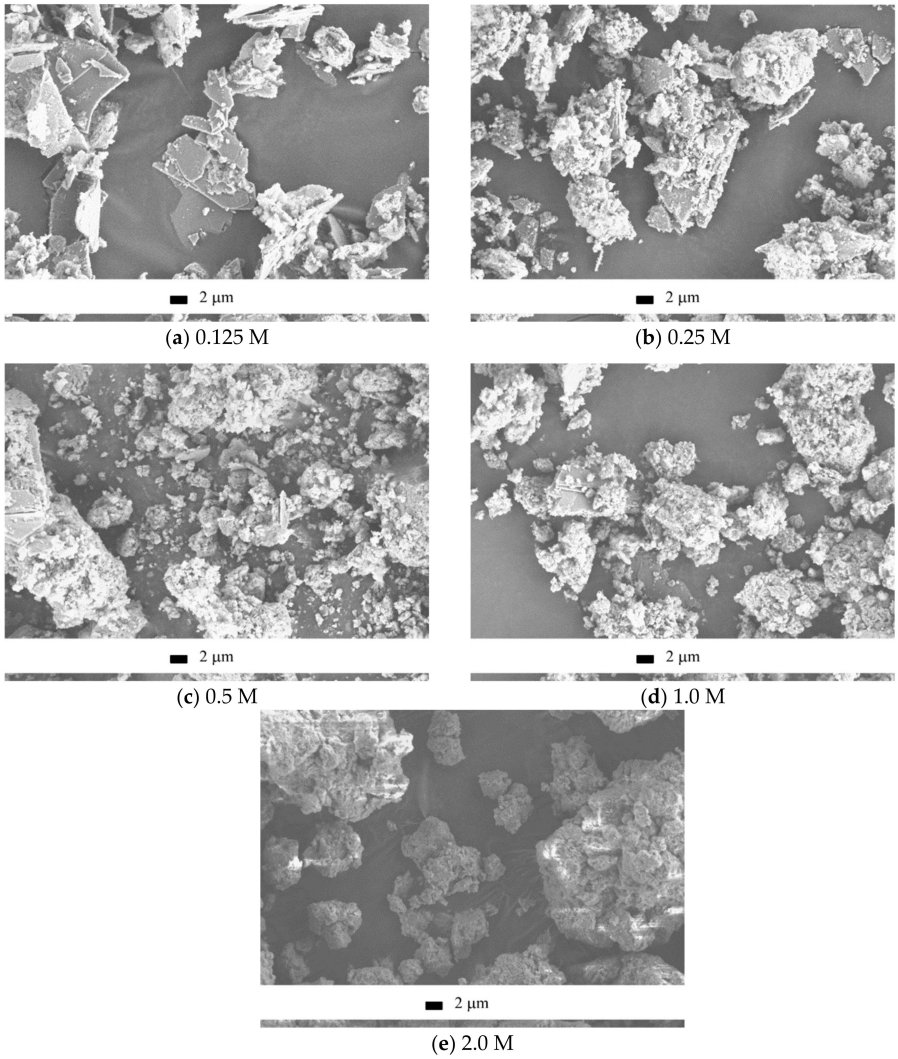

Figure 4. SEM images of the powders synthesized from aqueous solutions of $Ca(CH_3COO)_2$ and $(NH_4)_2HPO_4$ at Ca/P = 1.5. Calcium acetate concentration: 0.125 (**a**), 0.25 (**b**), 0.5 (**c**), 1.0 (**d**), and 2.0 (**e**).

The collected TA data (Figure 6) revealed that total mass loss of the as-prepared powders upon heating to 1000 °C ranged between about 20% (the "0.25 M" sample) and 40% (the "2 M" sample).

The highest mass loss for the powder prepared from the most concentrated solutions was evidently due to high content of the reaction by-product in the sample. The specific smell of the powder suggested that the by-product contained acetic acid and/or ammonium acetate, even though the corresponding reflexes were not observed in the XRD pattern. Ammonium acetate could be adsorbed at the powder surface from the mother liquor during synthesis. The effect of the precursors concentration during calcium phosphates synthesis on the by-product(s) content in the prepared powder from has been shown earlier as well [8]. The presence of brushite caused steep mass loss at 200 °C for the powders prepared using 0.125 and 0.25 M calcium acetate solutions; the mass loss at 200 °C was more prominent in the case of the more dilute precursor solution. On the other hand, the TG curve for the powder prepared from the most concentrated precursor solution (2 M) resembled that for Ca-deficient hydroxyapatite $Ca_9(HPO_4)(PO_4)_5(OH)$ [13,36], exhibiting a typical bend at 700–750 °C. The TG curves for the "0.5 M" and "1.0 M" powders were in between the above-described extreme cases, exhibiting intermediate mass losses both at 200 and 1000 °C.

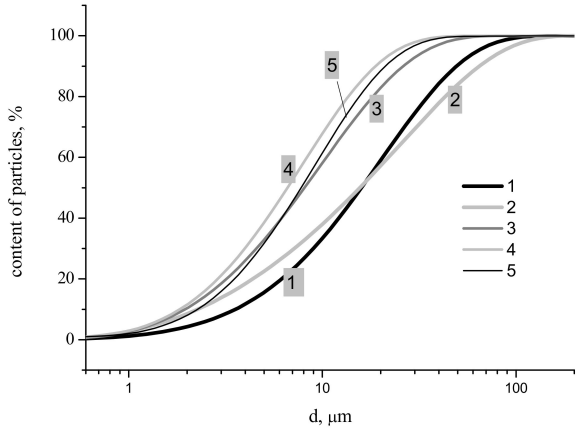

(**a**)

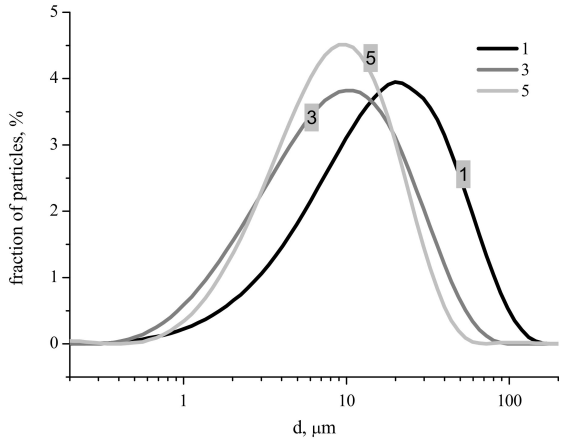

(**b**)

Figure 5. Integral (**a**) and differential (**b**) curves of the particles size distributions of the powders synthesized from aqueous solutions of $Ca(CH_3COO)_2$ and $(NH_4)_2HPO_4$ at Ca/P = 1.5. Calcium acetate concentration: 2.0 M (**1**), 1.0 M (**2**), 0.5 M (**3**), 0.25 M (**4**), and 0.125 M (**5**).

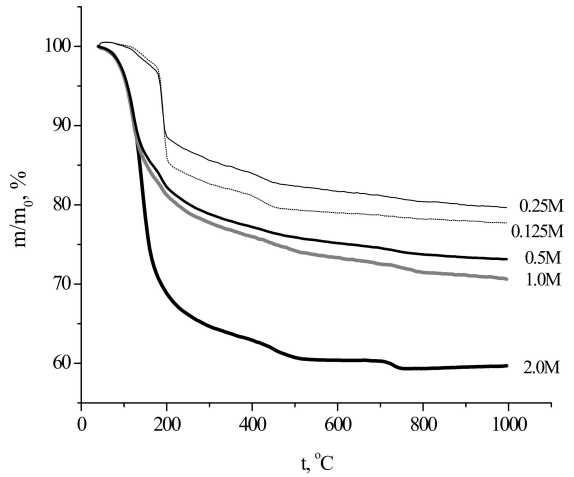

Figure 6. Thermal analysis (TA) curves of the as-prepared powder samples synthesized from aqueous solutions of $Ca(CH_3COO)_2$ and $(NH_4)_2HPO_4$ at Ca/P = 1.5. Calcium acetate concentration is shown near the corresponding curves.

The simultaneously recorded mass spectra (MS) profiles (Figure 7) of the gases evolved during the heat treatment showed that H_2O (m/z 18, Figure 7a) gave the major contribution to the mass loss of the powders.

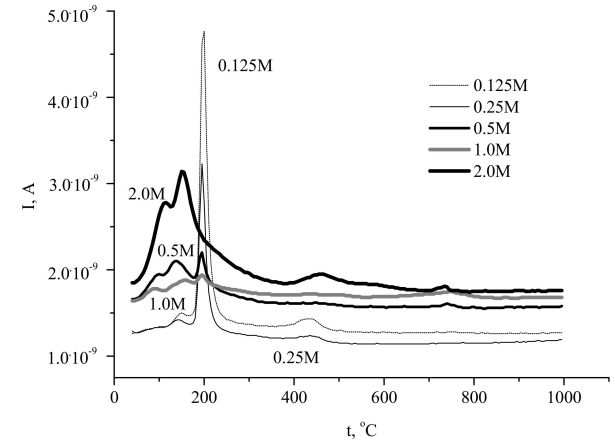

m/z = 18 (**a**)

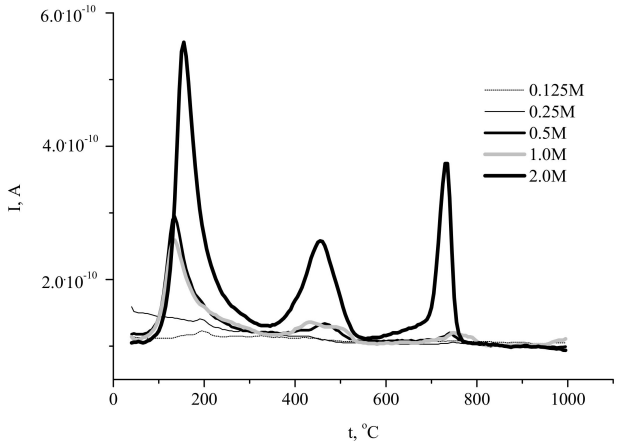

m/z = 44 (**b**)

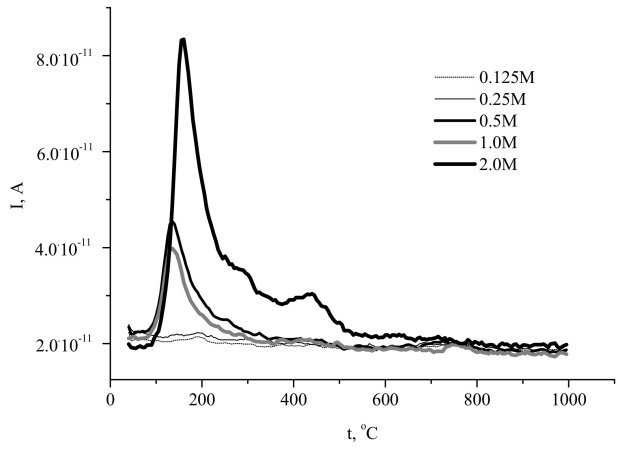

m/z = 30 (**c**)

Figure 7. Mass spectra MS profiles of the evolved gaseous decomposition products of the as-prepared powder samples synthesized from aqueous solutions of $Ca(CH_3COO)_2$ and $(NH_4)_2HPO_4$ at Ca/P = 1.5. Calcium acetate concentration is shown in the legend; m/z: 18 (**a**), 44 (**b**), 30 (**c**).

The profiles of water evolution could be divided into three types. The first one reflected the decomposition of brushite phase with prominent signals at 200 and 400 °C (the "0.125 M" and "0.25 M" powders). Another shape of the curve corresponded to the decomposition of Ca-deficient hydroxyapatite (the "2 M" powder). Other samples showed the intermediate type curves of water evolution during decomposition, containing the peaks typical of both brushite and calcium deficient hydroxyapatite.

The profiles of carbon dioxide evolution (m/z 44, Figure 7b) from the synthesized powders reflected the contribution of ammonium acetate (CH_3COONH_4) decomposition to the heat-induced mass loss of the samples. As seen in Figure 7b, the evolution of CO_2 from the powders prepared from 0.5–2.0 M calcium acetate solutions occurred in three stages with the maximums observed at 130–150, 430–470, and 730–750 °C.

It should be noted that evolution of CO_2 was negligibly weak for the powders prepared using more dilute precursor solutions (0.125–0.25 M), due to the low content of the reaction by-product in the samples. The presence of three maximums revealed the complex pathway of the organic by-product decomposition. Obviously, the transformations of ammonium acetate yielded a mixture of various carbonaceous solids, their ratio being changed during heating at 400–800 °C. The presence of carbonaceous species (including carbon) in the solid residue was confirmed by the observed evolution of the sample color during heating. Likely, the color of calcium phosphates powder was determined by the presence of the products of partial decomposition over the lower temperature range and by amorphous carbon at intermediate temperature, whereas carbon was completely removed during the third stage of decomposition.

Heating of ammonium compounds in the presence of oxygen can lead to the formation of different nitrogen oxides via a complex multistage process. In this study, we report the data for NO evolution (m/z 30). The corresponding profiles (Figure 7c) showed that elimination of NO from the powder prepared at the highest concentration of the precursor (2 M) occurred over a broad temperature range (80–700 °C) with a sharp peak at 160 °C, whereas in the case of the products obtained at intermediate precursor concentrations the range of NO evolution was narrower: Up to 350 °C ("1 M") and up to 320 °C ("0.5 M"), with sharp peaks at about 135 °C. No noticeable evolution of NO was detected for the powders prepared at lower precursor concentrations. Hence, the amount of the evolved NO and the range of its evolution were expectedly affected by the amount of the reaction by-product in the synthesized powder. Let us mention that some of the maximums in the "m/z 30" curves coincided with those in the "m/z 18" profiles, while other peaks corresponded to those in the "m/z 44" traces. Therefore, various stages of NO evolution were accompanied by the formation of H_2O or CO_2, and the overall mass loss was a result of several competing multistage processes involving both calcium phosphate species and ammonium acetate. It has been earlier revealed [18,20,23,24,26] that the reaction by-product consisting of carboxylic acids and their ammonium salts undergoes partial and then complete decomposition at temperatures below 800 °C. Therefore, the calcium phosphates powders containing carboxylic acids or their salts (ammonium, sodium [37], or potassium [38]) heat-treated at 400–800 °C were black-colored due to the formation of carbon or products of partial decomposition of organic substances present in the as-prepared samples.

Rheological properties of the synthesized powders could be estimated from the density values of green compacted samples after pressing at 100 MPa (Figure 8).

The relative densities of the powder compacts were calculated based on the pycnometric density of calcium phosphate ceramic samples after firing at 1100 °C for 2 h. The relative densities of the powder compacts fabricated from the powders synthesized from more dilute precursor solutions (0.125–0.5 M) were about 37% to 39%. The relative densities of the powder compacts fabricated from the powders prepared from more concentrated precursor solutions (1 and 2 M) were about 44% and 57%, respectively. We suppose that the achievable density of the powder compact was related to the morphology of the powder particles (Figure 4) and the presence of the reaction by-product in the synthesized powders after disaggregation. In the case of the studied powders, ammonium acetate

played the role of temporary technological binder facilitating sliding of the particles to form a denser package. Indeed, the samples of the "2 M" powder compacted by pressing had the highest green density, coinciding with the fact that it consisted of isometric particles and contained the highest amount of the reaction by-product.

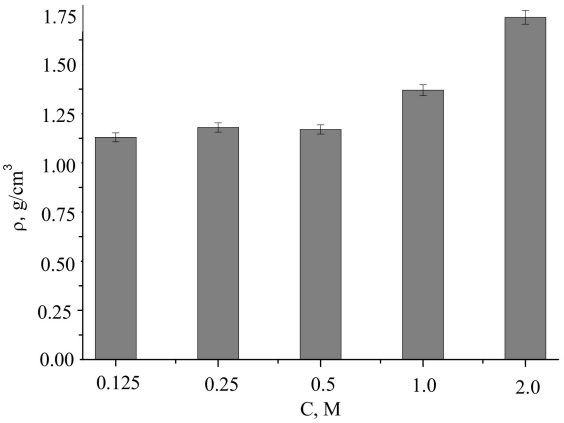

Figure 8. The density of the green powder compacts pressed at 100 MPa. The labels at the horizontal axis show the concentration of $Ca(CH_3COO)_2$ solution used for the synthesis.

XRD patterns of the compacted powder specimens heat-treated at 1100 °C are given in Figure 9.

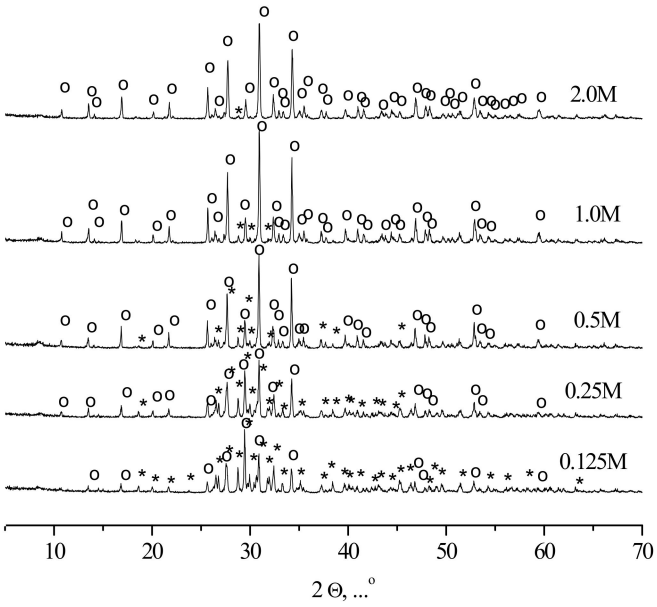

Figure 9. XRD patterns of the ceramic samples prepared from the synthesized powders after firing at 1100 °C. Concentrations of $Ca(CH_3COO)_2$ precursor are shown near the curves. o—β-$Ca_3(PO_4)_2$, PDF card # 1-169; *—β-$Ca_2P_2O_7$, PDF card # 9-346.

According to the XRD data, tricalcium phosphate β-$Ca_3(PO_4)_2$ (PDF card # 1-169) and calcium pyrophosphate β-$Ca_2P_2O_7$ (PDF card # 9-346) were present in ceramic samples, fabricated from synthesized powders. The sample corresponding to the highest precursor concentration ("2 M") contained exclusively tricalcium phosphate β-$Ca_3(PO_4)_2$ after the heat treatment, the sample fabricated from the "0.125 M" powder consisted preferably of calcium pyrophosphate β-$Ca_2P_2O_7$, whereas the

intermediate ceramic samples revealed the presence of both tricalcium phosphate β-$Ca_3(PO_4)_2$ and calcium pyrophosphate β-$Ca_2P_2O_7$ phases with the regularly changing reflexes intensities.

The formation of calcium pyrophosphate β-$Ca_2P_2O_7$ could be expressed by Reactions (3) and (4):

$$CaHPO_4 \cdot 2H_2O \rightarrow CaHPO_4 + 2H_2O. \quad (3)$$

$$2CaHPO_4 \rightarrow Ca_2P_2O_7 + H_2O. \quad (4)$$

The formation of tricalcium phosphate β-$Ca_3(PO_4)_2$ which could be treated as dominated phase for the "2 M" powder was explained by Reactions (5) and (6) or Reactions (5), (6), (8) and (10) for other powders:

$$Ca_9(HPO_4)(PO_4)_5(OH) \rightarrow 3Ca_3(PO_4)_2 + H_2O.$$

$$Ca_{10}(PO_4)_6(OH)_2 + Ca_2P_2O_7 \rightarrow 4Ca_3(PO_4)_2 + xH_2O. \quad (6)$$

$$Ca(CH_3COO)_2 + 2O_2 \rightarrow CaCO_3 + 3H_2O + CO_2. \quad (7)$$

$$Ca_2P_2O_7 + CaCO_3 \rightarrow Ca_3(PO_4)_2 + CO_2. \quad (8)$$

$$CaCO_3 \rightarrow CaO + CO_2. \quad (9)$$

$$Ca_2P_2O_7 + CaO \rightarrow Ca_3(PO_4)_2. \quad (10)$$

The presence of CaO in the powder compact at high temperature could be due to the transformations of the $Ca(CH_3COO)_2$ admixture (Reactions (6) and (8)). In turn, $Ca(CH_3COO)_2$ admixture was a result of the formation of brushite (with Ca/P = 1) from the mixtures of the nominal composition corresponding to Ca/P = 1.5. Indeed, the Ca/P = 1.5 starting conditions correspond to the excess of $Ca(CH_3COO)_2$ according to Equation (1).

The content of the phases in the ceramic samples prepared from the synthesized powders after firing at 1100 °C are presented in Figure 10. The content of the β-$Ca_3(PO_4)_2$ phase in the ceramic samples increases with increasing of concentration of starting solutions and after firing at 1100 °C for ceramics based on powder synthesized from solution with 2 M concentration of $Ca(CH_3COO)_2$ reaches 95%.

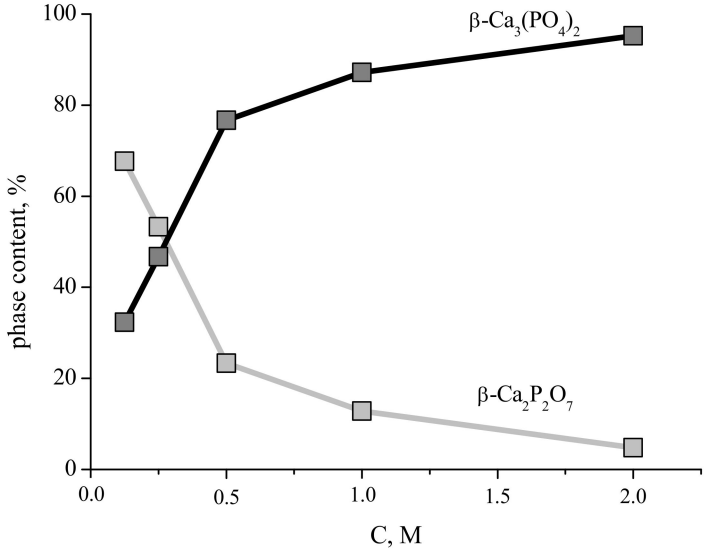

Figure 10. The content of the phases in the ceramic samples prepared from the synthesized powders after firing at 1100 °C; the labels at the horizontal axis show the concentration of $Ca(CH_3COO)_2$ solution used for the synthesis.

Relative diameter and mass (with respect to those of the compacted sample before the heat treatment) of the ceramic samples as functions of the $Ca(CH_3COO)_2$ concentration in the starting solution are presented in Figure 11.

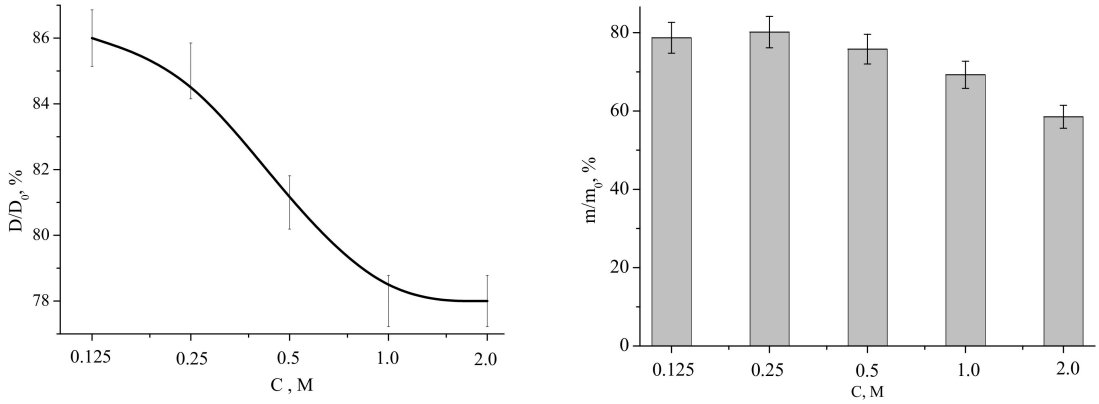

(**a**) (**b**)

Figure 11. Relative diameter (**a**) and mass (**b**) of ceramic samples after firing at 1100 °C: *D* and *m*—diameter and mass of a sample after firing at 1100 °C, respectively; D_0 and m_0—diameter and mass of the corresponding green powder compacts before firing; the labels at the horizontal axis show the concentration of $Ca(CH_3COO)_2$ solution used for the synthesis.

The relative diameter dependence was decreasing, showing the lowest value (linear shrinkage of 22%) for the samples fabricated from the "1 M" and "2 M" powders. The highest relative diameter (the lowest liner shrinkage of 14%) was observed for the sample prepared from the "0.125 M" powder. The mass loss of the powders after firing at 1100 °C for 2 h was within the 22% to 42% range, coinciding with the TA data (Figure 6).

The densities of the compacted powder samples and after firing at 1100 °C were of 1.4–2.2 g/cm^3, increasing with the concentration of the precursor used for the powder preparation (Figure 12).

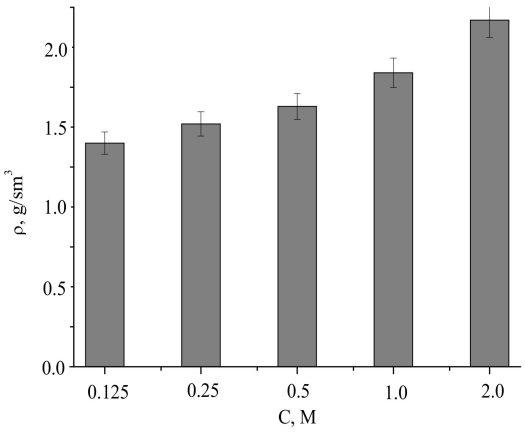

Figure 12. Density of the ceramic samples after firing at 1100 °C. The labels at the horizontal axis show the concentration of $Ca(CH_3COO)_2$ solution used for the synthesis.

Assuming pycnometric density of samples after firing at 1100 °C, the measured densities of the ceramics corresponded to 46% to 70% of the theoretical values.

The microstructure of the ceramic materials after annealing at 1100 °C (Figure 13) coincided with the discussed trends of the relative diameter and density.

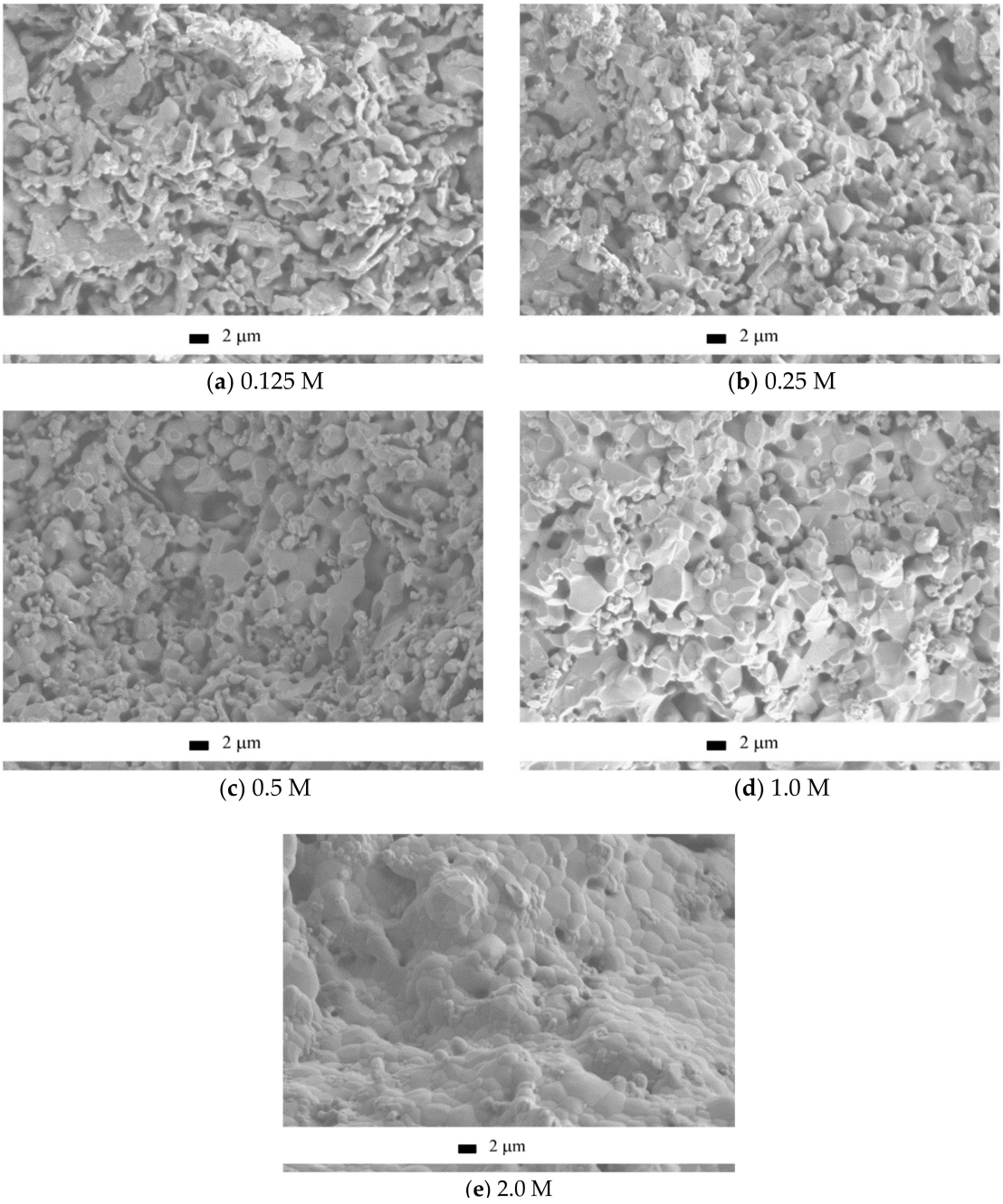

Figure 13. SEM images of the ceramic materials based on powders synthesized from aqueous solutions of $Ca(CH_3COO)_2$ and $(NH_4)_2HPO_4$ at Ca/P = 1.5 after firing at 1100 °C. Calcium acetate concentration: 0.125 (**a**), 0.25 (**b**), 0.5 (**c**), 1.0 (**d**), and 2.0 M (**e**).

The microstructure of the ceramics fabricated from the "0.125 M", "0.25 M", "0.5 M", and "1 M" powders looked "undersintered," containing 0.5–4 μm pores and 0.5–4 μm grains, partially plate-shaped. It should be noted that the fraction of coarse grains in the sample grew with the increase in the $Ca(CH_3COO)_2$ concentration in the starting solution. The microstructure of ceramics fabricated from the "2 M" powder looked different, being quite uniform. The constituting grains were of 0.5–3 μm, predominantly of 2–3 μm. The difference in the microstructure of the ceramics based on calcium pyrophosphate and that containing majorly tricalcium phosphate can be explained by lower staring powder compact density, plate morphology of the brushite particles and possibly by low mobility of the pyrophosphate ions during the solid-state sintering [39,40].

4. Conclusions

Comprehensive investigation of calcium phosphate powders prepared via a wet-precipitation route from aqueous solutions of calcium acetate and ammonium hydrophosphate revealed strong effects of the concentration of the starting solutions on the pH evolution during the synthesis, phase composition and microstructure of the as-synthesized products and even the ceramics based on them, despite the fact that by-products and admixtures were completely eliminated during the firing. In detail, heat treatment of the powder compacts at 1100 °C afforded the products containing exclusively the biocompatible phases: Calcium pyrophosphate and tricalcium phosphate. Therefore, the discussed method can be recommended as a process stage for the production of resorbable phosphate bioceramics with desired phase composition and microstructure.

Author Contributions: Conceptualization, T.S. (Tatiana Safronova); Methodology, T.S. (Tatiana Safronova); Data curation, V.P.; Formal analysis, V.P.; Investigation, T.S. (Tatiana Safronova), V.P., Y.F., T.S. (Tatiana Shatalova), E.K., D.L., G.K. and Y.S.; Visualization, Y.F. and T.S. (Tatiana Safronova); Writing—original draft, T.S. (Tatiana Safronova) and E.K.; Writing—review & editing, T.S. (Tatiana Safronova); Supervision, T.S. (Tatiana Safronova); Project administration, T.S. (Tatiana Safronova).

Funding: This research was funded by RUSSIAN SCIENCE FOUNDATION, grant number 15-19-00103.

Acknowledgments: The experiments were performed using the equipment purchased in the scope of the Program of Development of Lomonosov Moscow State University.

Conflicts of Interest: The authors declare no conflict of interest.

References

1. Hench, L.L. Bioceramics: From Concept to Clinic. *J. Am. Ceram. Soc.* **1991**, *74*, 1487–1510. [CrossRef]
2. Yu, X.; Tang, X.; Gohil, S.V.; Laurencin, C.T. Biomaterials for Bone Regenerative Engineering. *Adv. Healthc. Mater.* **2015**, *4*, 1268–1285. [CrossRef] [PubMed]
3. Safronova, T.V.; Putlyaev, V.I. Powder Systems for Calcium Phosphate Ceramics. *Inorg. Mater.* **2017**, *53*, 17–26. [CrossRef]
4. Lin, K.; Wu, C.; Chang, J. Advances in synthesis of calcium phosphate crystals with controlled size and shape (Review). *Acta Biomater.* **2014**, *10*, 4071–4102. [CrossRef] [PubMed]
5. Brown, P.W. Phase Relationships in the Ternary System CaO-P_2O_5-H_2O at 25 °C. *J. Am. Ceram. Soc.* **1992**, *75*, 17–22. [CrossRef]
6. Liu, C.; Huang, Y.; Shen, W.; Cui, J. Kinetics of hydroxyapatite precipitation at pH 10 to 11. *Biomaterials* **2001**, *22*, 301–306. [CrossRef]
7. Raynaud, S.; Champion, E.; Bernasche-Assollant, D.; Thomas, P. Calcium phosphate apatites with variable Ca/P atomic ratio I. Synthesis, characterization and thermal stability of powder. *Biomaterials* **2002**, *2*, 1065–1072. [CrossRef]
8. Safronova, T.V.; Shekhirev, M.A.; Putlyaev, V.I.; Tret'yakov, Y.D. Hydroxyapatite-based ceramic materials prepared using solutions of different concentrations. *Inorg. Mater.* **2007**, *43*, 901–909. [CrossRef]
9. Safronova, T.V. Phase composition of ceramic based on calcium hydroxyapatite powders containing byproducts of the synthesis reaction. *Glass Ceram.* **2009**, *66*, 136–139. [CrossRef]
10. Suvorova, E.I.; Polyak, L.E.; Komarov, V.F.; Melikhov, I.V. Study of synthetic hydroxyapatite by the method of high-resolution transmission electron microscopy: Morphology and growth direction. *Crystallogr. Rep.* **2000**, *45*, 857–861. [CrossRef]
11. Anwar, A.; Kanwal, Q.; Akbar, S.; Munawar, A.; Durrani, A.; Hassan Farooq, M. Synthesis and characterization of pure and nanosized hydroxyapatite bioceramics. *Nanotechnol. Rev.* **2017**, *6*, 149–157. [CrossRef]
12. Kalita, S.J.; Verma, S. Nanocrystalline hydroxyapatite bioceramic using microwave radiation: Synthesis and characterization. *Mater. Sci. Eng. C* **2010**, *30*, 295–303. [CrossRef] [PubMed]
13. Safronova, T.V.; Putlyaev, V.I.; Avramenko, O.A.; Shekhirev, M.A.; Veresov, A.G. Ca-deficient hydroxyapatite powder for producing tricalcium phosphate based ceramics. *Glass Ceram.* **2011**, *68*, 28–32. [CrossRef]

14. Minh, D.P.; Rio, S.; Sharrock, P.; Sebei, H.; Lyczko, N.; Tran, N.D.; Raii, M.; Nzihou, A. Hydroxyapatite starting from calcium carbonate and orthophosphoric acid: Synthesis, characterization, and applications. *J. Mater. Sci.* **2014**, *49*, 4261–4269. [CrossRef]
15. Türk, S.; Altınsoy, İ.; ÇelebiEfe, G.; Ipek, M.; Özacar, M.; Bindal, C. Microwave-assisted biomimetic synthesis of hydroxyapatite using different sources of calcium. *Mater. Sci. Eng. C* **2017**, *76*, 528–535. [CrossRef] [PubMed]
16. Safronova, T.V.; Kuznetsov, A.V.; Korneychuk, S.A.; Putlyaev, V.I.; Shekhirev, M.A. Calcium phosphate powders synthesized from solutions with $[Ca^{2+}]/[PO_4{}^{3-}] = 1$ for bioresorbable ceramics. *Cent. Eur. J. Chem.* **2009**, *7*, 184–191. [CrossRef]
17. Safronova, T.; Putlayev, V.; Shekhirev, M. Resorbable calcium phosphates based ceramics. *Powder Metall. Met. Ceram.* **2013**, *52*, 357–363. [CrossRef]
18. Safronova, T.V.; Putlyaev, V.I.; Filippov, Y.Y.; Vladimirova, S.A.; Zuev, D.M.; Cherkasova, G.S. Synthesis of calcium-phosphate powder from calcium formiate and ammonium hydrophosphate for obtaining biocompatible resorbable biphase ceramic materials. *Glass Ceram.* **2017**, *74*, 185–190. [CrossRef]
19. Safronova, T.V.; Putlyaev, V.I.; Kazakova, G.K.; Korneichuk, S.A. Biphase $CaO–P_2O_5$ ceramic based on powder synthesized from calcium acetate and ammonium hydrophosphate. *Glass Ceram.* **2013**, *70*, 65–70. [CrossRef]
20. Safronova, T.V.; Mukhin, E.A.; Putlyaev, V.I.; Knotko, A.V.; Evdokimov, P.V.; Shatalova, T.B.; Filippov, Y.Y.; Sidorov, A.V.; Karpushkin, E.A. Amorphous calcium phosphate powder synthesized from calcium acetate and polyphosphoric acid for bioceramics application. *Ceram. Int.* **2017**, *43*, 1310–1317. [CrossRef]
21. White, E.W. Calcium Phosphate Bone Substitute Materials. U.S. Patent 4861733, 29 August 1989.
22. Chai, C.; Ben-Nissan, B.; Pyke, S.; Evans, L. Sol-gel derived hydroxylapatite coatings for biomedical applications. *Mater. Manuf. Process* **1995**, *10*, 205–216. [CrossRef]
23. Kiselev, A.S.; Safronova, T.V.; Putlyaev, V.I.; Kukueva, E.V.; Knot'ko, A.V. Synthesis of Nanocrystalline Calcium Phosphates from Calcium Propionate and Ammonium Phosphates. In Proceedings of the 28th European Conference on Biomaterials, Athens, Greece, 4–8 September 2017.
24. Safronova, T.V.; Putlyaev, V.I.; Andreev, M.D.; Filippov, Y.Y.; Knotko, A.V.; Shatalova, T.B.; Evdokimov, P.V. Synthesis of calcium phosphate powder from calcium lactate and ammonium hydrogen phosphate for the fabrication of bioceramics. *Inorg. Mater.* **2017**, *53*, 874–884. [CrossRef]
25. Pandey, A.; Aswath, P. Microwave-Assisted in Situ Synthesis of Poly L-Lactic Acid with Nanoparticles of Calcium Phosphate. *Int. Int. J. Polym. Mater. Polym. Biomater.* **2010**, *59*, 911–922. [CrossRef]
26. Safronova, T.V.; Putlyaev, V.I.; Sergeeva, A.I.; Kunenkov, E.V.; Tret'yakov, Y.D. Synthesis of nanocrystalline calcium hydroxyapatite from calcium saccharates and ammonium hydrogen phosphate. *Dokl. Chem.* **2009**, *426*, 118–123. [CrossRef]
27. Safronova, T.V.; Kazakova, G.K.; Evdokimov, P.V.; Shatalova, T.B.; Knotko, A.V.; Korotkova, A.V.; Putlyayev, V.I. Ceramics Based on Calcium Phosphate Powder Synthesized from Calcium Saccharate and Ammonium Hydrophosphate. *Inorg. Mater. Appl. Res.* **2016**, *7*, 635–640. [CrossRef]
28. Msagati, T.A.M. *The Chemistry of Food Additives and Preservatives*; John Wiley & Sons: Chichester, UK, 2012; pp. 125–130, ISBN 978-1-118-27414-9.
29. Perrin, D.D. *Buffers for pH and Metal Ion Control*; Springer Science & Business Media: London, UK, 1974; pp. 1–122, ISBN 13:978-0-412-21890-3.
30. Gustafsson, J.P. Visual MINTEQ version 3.1, Department of Sustainable Development//Environmental Science and Engineering, KTH, Stockholm, 2013. Available online: https://vminteq.lwr.kth.se/ (accessed on 14 December 2018).
31. ICDD (2010). PDF-4+ 2010 (Database), Edited by Dr. Soorya Kabekkodu, International Centre for Diffraction Data, Newtown Square, PA, USA. Available online: http://www.icdd.com/products/pdf2.htm (accessed on 14 December 2018).
32. Christoffersen, J.; Christoffersen, M.R.; Kibalczyc, W.; Andersen, F.A. A contribution to the understanding of the formation of calcium phosphates. *J. Cryst. Growth* **1989**, *94*, 767–777. [CrossRef]
33. Abbona, F.; Baronnet, A. A XRD and TEM study on the transformation of amorphous calcium phosphate in the presence of magnesium. *J. Cryst. Growth* **1996**, *165*, 98–105. [CrossRef]
34. Brečević, L.; Füredi-Milhofer, H. Precipitation of Calcium Phosphates from Electrolyte Solutions II. The Formation and Transformation of the Precipitates. *Calcif. Tissue Res.* **1972**, *10*, 82–90. [CrossRef] [PubMed]

35. Traven, V.F. Organic Chemistry: Textbook. In *Akademkniga*; Russian Federation: Moscow, Russia, 2004; Volume 2, p. 146. 583p, ISBN 5-94628-172-0.
36. Vallet-Regi, M.; Rodriguez-Lorenzo, L.M.; Salinas, A.J. Synthesis and characterization of calcium deficient apatite. *Solid State Ionics* **1997**, *101–103*, 1279–1285. [CrossRef]
37. Safronova, T.V.; Putlyaev, V.I.; Kuznetsov, A.V.; Ketov, N.A.; Veresov, A.G. Properties of calcium phosphate powder synthesized from calcium acetate and sodium hydrophosphate. *Glass Ceram.* **2011**, *68*, 131–135. [CrossRef]
38. Safronova, T.V.; Korneichuk, S.A.; Putlyaev, V.I.; Boitsova, O.V. Ceramics made from calcium hydroxyapatite synthesized from calcium acetate and potassium hydrophosphate. *Glass Ceram.* **2008**, *65*, 28–32. [CrossRef]
39. Safronova, T.V.; Putlyaev, V.I.; Shekhirev, M.A.; Kuznetsov, A.V. Composite ceramic containing a bioresorbable phase. *Glass Ceram.* **2007**, *64*, 102–106. [CrossRef]
40. Kim, D.W.; An, J.S.; Cho, I.S. Effects of Mg and Sr co-addition on the densification and biocompatible properties of calcium pyrophosphate. *Ceram. Int.* **2018**, *44*, 9689–9695. [CrossRef]

© 2018 by the authors. Licensee MDPI, Basel, Switzerland. This article is an open access article distributed under the terms and conditions of the Creative Commons Attribution (CC BY) license (http://creativecommons.org/licenses/by/4.0/).